International Journal of Thermal Sciences 48 (2009) 1988–1996

Contents lists available at ScienceDirect

International Journal of Thermal Sciences

journal homepage: www.elsevier.com/locate/ijts

Parametric evaluation of refrigerated air curtains for thermal insulation

Yun-Guang Chen

Department of Refrigeration and Cryogenic Engineering, School of Energy and Power Engineering, Xi'an Jiaotong University, Xianning west road 28, Xi'an, Shaanxi 710049, PR China

ARTICLE INFO

Article history:
Received 16 August 2008
Received in revised form
9 March 2009
Accepted 10 March 2009
Available online 3 April 2009

Keywords:
Refrigerated air curtain
Thermal insulation
Sealing ability

ABSTRACT

The refrigerated air curtain used for cavity insulation in the present study is an idealization of the refrigerated air curtain used in supermarket food display cabinets. The thermal insulation performance of refrigerated air curtains is very important for perishable food storage and energy saving for refrigerated display cabinets. Thermal insulation ability of recirculated refrigerated air curtains was numerically studied in the present work. The results show that the refrigerated air curtains are negatively buoyant jets and tend to flow toward the inside cabinet due to stack pressure, so the initial momentum must be sufficiently large to sustain the pressure difference across the air curtain and assure the thermal insulation. The length–width ratio and the discharge angle of the air curtains, the height–depth ratio of the cavity and the dimension and position of the inside shelves would greatly influence the thermal insulation performance of air curtains, therefore were extensively discussed. The maximum Richardson numbers or the optimum parameter selections in each situation were presented for practical design of refrigerated air curtains used in multi-deck display cabinets.

1. Introduction

Open-type multi-deck refrigerated display cabinets are widely used in supermarkets and grocery stores due to good display effect and allowing customers conveniently access to the inside food. Refrigerated air curtains are used in display cabinets as replacements for glass doors to prevent the penetration of ambient warmer air, therefore account for a considerable proportion of the energy used in supermarkets [1]. So the performance of air curtains is very crucial for food storage and energy saving. However, the characteristics of air curtains are very complex and not well understood yet. So it is quite difficult for engineers to design or choose appropriate parameters in many different situations.

Many researchers have studied the performance of refrigerated display cabinets and air curtains. Earlier studies generally focused on the cooing load of the refrigerated display cabinets and several factors which have great effects on the performance of the air curtains, such as the temperature, humidity and air flow velocity of the ambient environment, the supply velocity and temperature of the air curtains, and the dimensions of the supply and return air grille [2–4]. In recent years, with the development of computational fluid dynamics (CFD) simulation and the experimental techniques, flow characteristics and more detailed information of the air curtains can be obtained from these approaches. Stribling et al. [5] carried out CFD simulation with refrigerated display cabinet and discussed the air curtain flow path and sensible cooling load. Different turbulence models and discretization schemes were compared for checking the effectiveness of the computational method. Cortella et al. [6] used the finite element method to analyze the air flow pattern and the temperature distribution inside the display cabinet. The effect of the different velocities in the double-band air curtain on the cooling load was considered in their study. D'Agaro et al. [7] showed that the 3-D simulation is very necessary for short cabinets in order to consider the end-wall effects. Field and Loth [8] and Kalluri [9] idealized the air curtain in fully loaded display cabinets as negatively buoyant wall jets, and used the particle image velocimetry (PIV) techniques to study the entrainment characteristics of air curtains. They observed the flow features of air curtains with Reynolds numbers ranging from 1500 to 8500, and quantified the effects of the Reynolds number and the Richardson number on the entrainment rates. They also observed the vortex development in the shear layer and indicated the ways to reduce the entrainment rate. Bhattacharjee and Loth [10] used the direct numerical simulation (DNS) method and Reynolds average navier–stokes (RANS) method to predict the momentum and thermal entrainment rates. The effects of different initial velocity profiles were also analyzed. Navaz et al. [11,12] combined computational and experimental methods to study the air entrainment of air curtains at different discharge temperature and velocities. Amin et al. [13] made a quite valuable contribution to use the trace gas technique to directly measure the infiltration rate of refrigerated air curtains.

E-mail address: ygchen@gmail.com

1290-0729/$ – see front matter © 2009 Elsevier Masson SAS. All rights reserved.
doi:10.1016/j.ijthermalsci.2009.03.003

Nomenclature

A	area (m^2)
b	width of initial air curtain (m)
D	depth of the cavity (m)
D_h	horizontal distance between the inner edge of the discharge grille and the front edge of the shelves (m)
D_v	vertical distance between neighboring shelves (m)
H	height of the cavity (m)
g	gravitational acceleration ($m\,s^{-2}$)
Gr	Grashof Number
L	length of the air curtain (m)
l	turbulence length scale (m)
ΔP_o	Total pressure difference across the air curtain (Pa)
ΔP_a	self-generated pressure difference across the air curtain (Pa)
ΔP_s	pressure difference across the air curtain due to temperature difference (Pa)
Ri	Richardson Number
Re	Reynolds Number
T	temperature (K)
Ti	turbulence intensity
u	mean velocity ($m\,s^{-1}$)
$\dot{V}$	volumetric entrainment rate ($m^3\,s^{-1}$)

Greek symbols

Θ	dimensionless temperature
ρ	density ($kg\,m^{-3}$)
ν	kinematic viscosity ($m^2\,s^{-1}$)
β	thermal expansion coefficient (K^{-1})
ϕ	generalized transport variables
Γ	effective diffusivity

Subscripts

amb	ambient
S	supply air
R	return air

However, to date, most results are case specific for both computational fluid dynamics (CFD) and experimental studies, so the results are not generally applicable and cannot be directly extended to practical designs for different dimensions and types. In addition, the effect of the inside shelves on the air curtain flow is seldom investigated. For vertical type display cabinets, the presence of shelves and stocked foodstuffs is helpful to the flow stability of air curtains [14], so the effect of inside shelves must be considered.

In order to get some general-purpose results, the present author idealized the actual problem as a cavity thermally insulated by a vertical single band cold air curtain, and proposed a maximum Richardson number (or a minimum Reynolds number) to assure the sealing ability of the air curtains [15]. The objective of the present paper is to study the parameter selections for design purpose based on our previous results, and the effect of the inside shelves is also quantitatively analyzed. Because the positions of shelves are random to some extent and the display cabinets are not always fully loaded, so it is necessary for air curtains themselves to maintain flow stability and thermal insulation performance for design considerations. Therefore, the empty cavity is first considered, and then the cavity with several shelves is further discussed in the present paper.

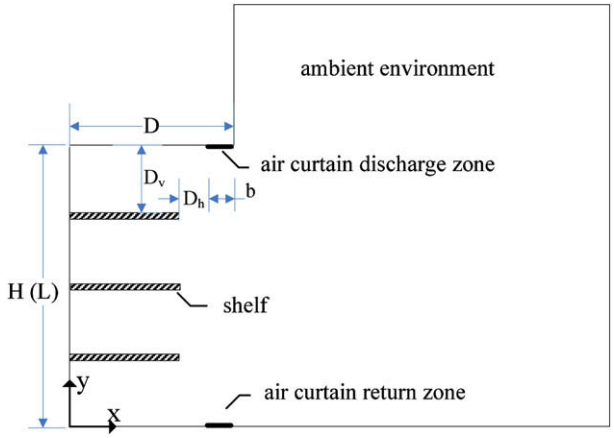

Fig. 1. Computational domain of the physical problem.

2. Physical and mathematical models

The calculation domain is shown in Fig. 1. The height and the depth of the cavity are H and D. There are discharge and return air zones at the top and bottom of the cavity adjacent to the ambient. When considering the effect of the shelves, it is assumed that the widths of the inside shelves are all same and the distances between neighboring shelves, D_v, are uniform. The shelves were assumed to be no thickness plates in calculation.

The height of the cavity, H (thus the length of the air curtain, L) is taken as the characteristic length, and the difference between ambient temperature T_{amb} and supplied air temperature T_S is used for non-dimensionalization of temperature. The non-dimensionalization scheme is as follows:

Non-dimensional temperature $\Theta = (T - T_S)/(T_{amb} - T_S)$; Grashof number $Gr = g\beta(T_{amb} - T_S)H^3/\nu_S^2$; Reynolds number $\mathrm{Re} = u_S H/\nu_S$; Richardson number $\mathrm{Ri} = Gr/\mathrm{Re}^2 = g\beta(T_{amb} - T_S)H/u_S^2$; Thermal entrainment factor $\alpha = (T_R - T_S)/(T_{amb} - T_S)$; Non-dimensional sensible cooling load due to convection $Q^* = \alpha\mathrm{Re}$ [10], which only accounts for the infiltration component, the largest part of the cooling load for multi-deck display cabinets.

The resulting equations for conservation of mass, momentum, energy, K and ε are represented by the following general equation:

$$\frac{\partial(\rho u\phi)}{\partial x} + \frac{\partial(\rho v\phi)}{\partial y} = \frac{\partial}{\partial x}\left(\Gamma_\phi \frac{\partial \phi}{\partial x}\right) + \frac{\partial}{\partial y}\left(\Gamma_\phi \frac{\partial \phi}{\partial y}\right) + S_\phi \quad (1)$$

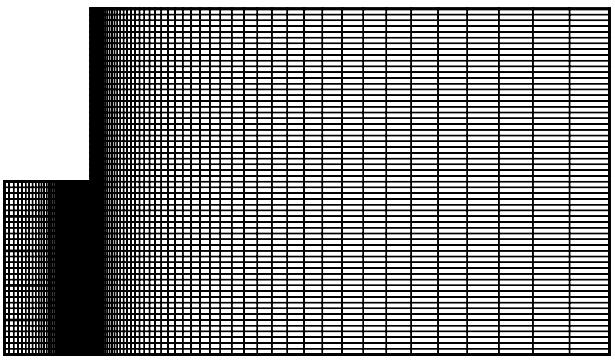

Fig. 2. Calculation grids.

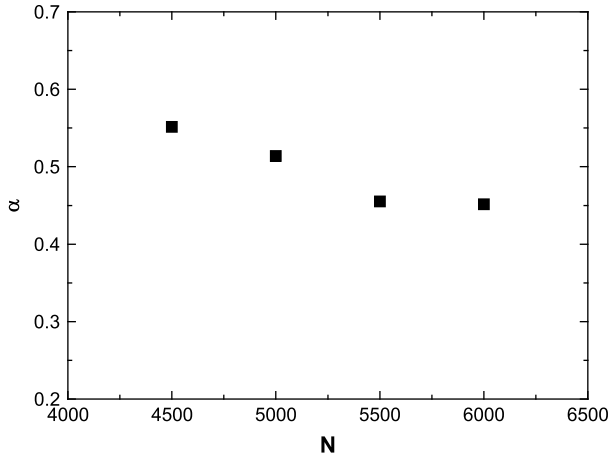

Fig. 3. The thermal entrainment factor α vs. the grid numbers.

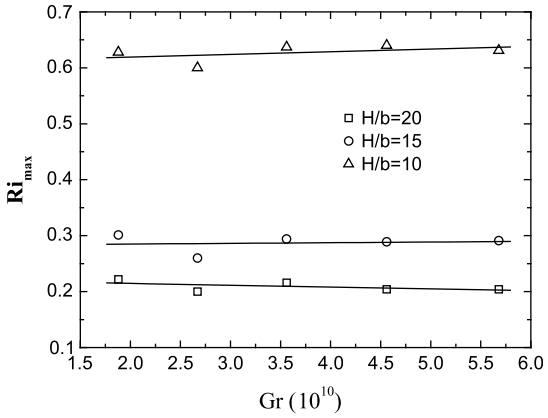

Fig. 5. Maximum Ri numbers for different H/b ratios.

The flow is assumed to be two dimensional because the length of the cabinets in end-to-end connection is often much larger than the dimensions of the air curtain. The buoyancy term is included in the momentum equations and the density variations are taken into account using the Boussinesq approximation for which the density is treated as a constant value in all solved equations except for the buoyancy term in the momentum equations, which is treated as

$$(\rho - \rho_0)g = \rho_0 g\beta(T - T_0) \tag{2}$$

The viscous dissipation is negligible and no radiative effects are considered. The equations were solved using the pressure-based, structured-grid, finite-volume method code FLUENT. The K–ε turbulence (RANS) model is used. The turbulent flow was calculated by SIMPLE algorithm and the second order upwind scheme was utilized for the approximation of the convection terms. Local refined grids are used along the entire length of the air curtain where the velocity and temperature gradients are very high, as shown in Fig. 2. The sensitivity of thermal entrainment factor α to the grid refinements is shown in Fig. 3.

Concerning the boundary conditions and the convergence condition, the turbulence intensities at the inlet were assumed to be 5 percent, from which the turbulence kinetic energy distribution and the dissipation rate inlet boundary condition were obtained as follows [16]:

$$k_{\text{inlet}} = \frac{3}{2}(u_{\text{inlet}}Ti)^2, \quad \varepsilon_{\text{inlet}} = C_\mu^{0.75}\frac{k_{\text{inlet}}^{3/2}}{l}, \quad l = 0.07\,b.$$

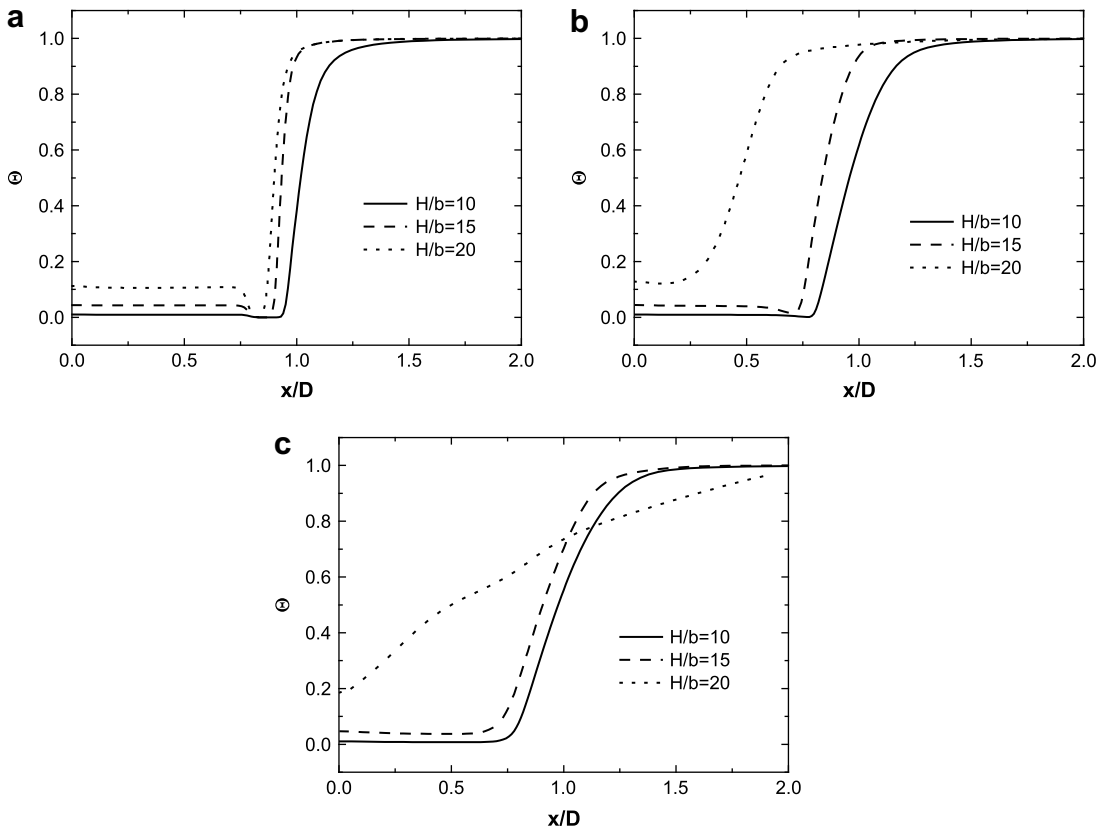

Fig. 4. Temperature distributions at different H/b ratios (Ri = 0.26): (a) $y/H = 0.9$; (b) $y/H = 0.5$; (c) $y/H = 0.1$.

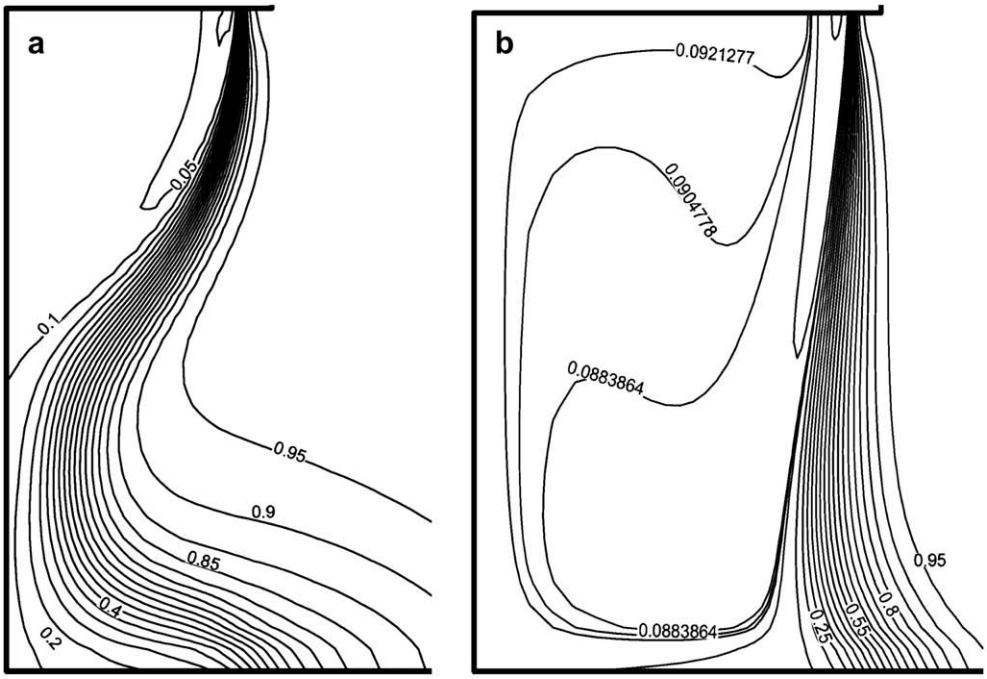

Fig. 6. Temperature distributions for different H/D ratios (Ri = 0.2, $H/b = 20$): (a) $H/D = 2.5$; (b) $H/D = 1.5$.

Where l is the turbulence length scale. The return air was assumed to be fully developed and the outflow condition was applied. The inside walls of the cavity and the shelves were adiabatic and non-slip boundary. For the enlarged environment boundaries, the pressure was equal to the ambient pressure and the ambient temperature was specified. A sufficiently large calculation domain was adopted so that the walls of the external medium do not have any influence on the flow of the air curtain and in the cavity. The convergence criterion is specified to absolute residuals $\leq 1.0 \times 10^{-6}$.

The volumetric entrainment rate is an important criterion to evaluate the performance of cold air curtains, from which the air flow through opening is obtained. Integrating the negative horizontal velocity over the opening will yield the volumetric entrainment rate as described in Ref. [11]:

$$\dot{V} = \int_{u<0} u \mathrm{d}A \tag{3}$$

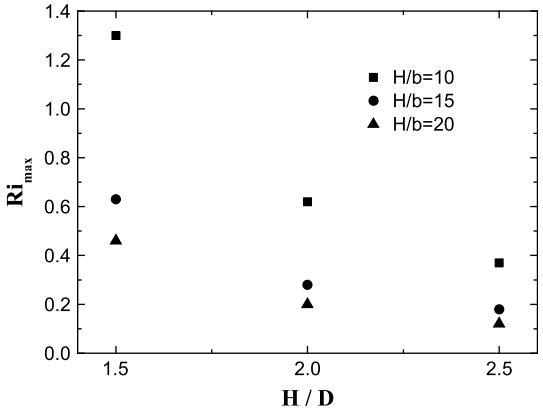

Fig. 7. Maximum Ri numbers for different H/D and H/b ratios.

3. Results and discussions

3.1. The effect of height–width ratios of the air curtains

Refrigerated air curtains are negatively buoyant jets, which combines the effects of forced and natural convection. Therefore, the air curtains must have enough momentum to sustain the pressure difference across the air curtains. Cold air curtain flows towards the inside cavity due to the pressure difference across the air curtain. The total pressure difference across the air curtain has two components:

$$\Delta P_o = \Delta P_a + \Delta P_s \tag{4}$$

Where ΔP_a is the self-generated pressure difference across the air curtain that occurs because of the momentum which is added to the inside cavity, and ΔP_s is the pressure difference due to the stack effect [17].

The perfect insulation of cold air curtains depends on the combined effects of initial momentum, gravitational forces and the pressure difference across the air curtain. If the initial momentum is insufficient to overcome the pressure difference, the cold air curtain will deflect inwards after exiting from the supply grille, and the insulation is not assured. The inside temperatures will rise and the volumetric infiltration rate will be very high. So for a given Grashof number there is a maximum Richardson number (or a minimum Reynolds number) to guarantee the thermal insulation for each cold air curtain [15].

The ratio of the opening height and the width of the initial air jet (height/width ratio) is an important factor that would influence the performance of air curtains. The present paper calculated and compared three different H/b ratios of 10, 15 and 20, which covers typical dimensions of refrigerated display cabinets. Fig. 4 shows the temperature distributions when the Richardson number equals 0.26. When the H/b ratio is 20, the air curtain will not work properly, and the temperatures at the middle and bottom parts deviate. The cold air curtains of small height/width ratios (i.e. shorter or thicker air curtains) show good insulation performance.

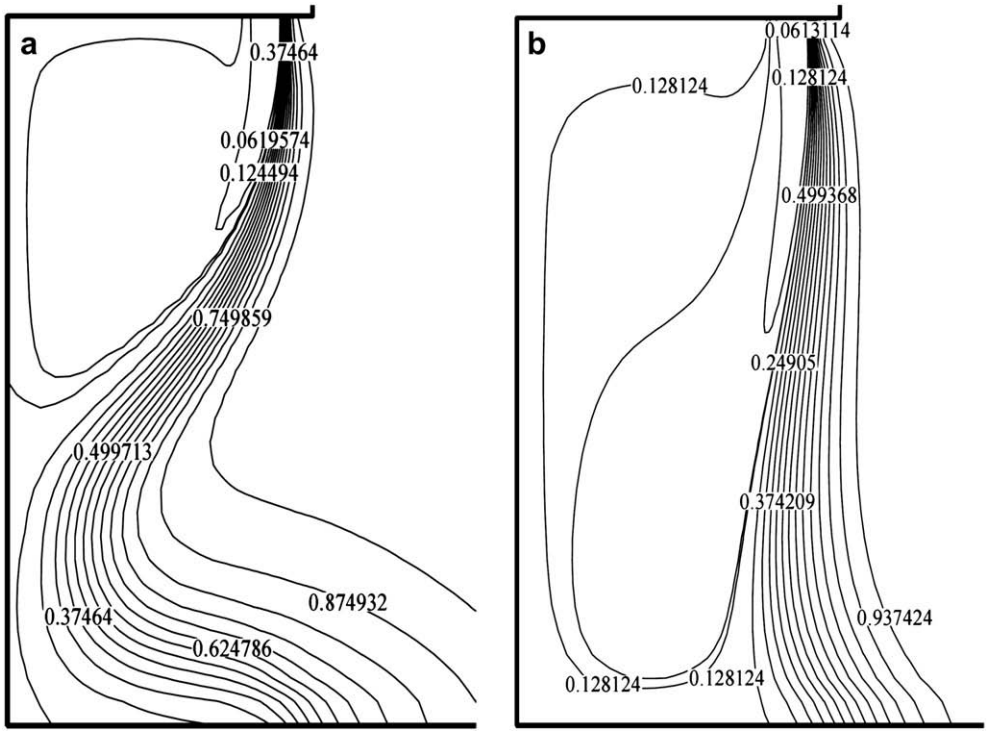

Fig. 8. Temperature distributions for different discharge angles (Ri = 0.26, $H/b = 20$): (a) $\theta = 5°$; (b) $\theta = 10°$.

Fig. 5 shows the maximum Richardson numbers that assure thermal insulation for different H/b ratios. The results show that for a given height/width ratio the maximum Richardson numbers maintain nearly constant for different Grashof numbers. For the cavity whose height/depth ratio equals 2 in the present study, the maximum Richardson numbers are 0.62, 0.28 and 0.20 for the height/width ratios of 10, 15 and 20 respectively. More detailed analyses of the effect of height–width ratios can be found in our previous results [15].

3.2. The effect of height–depth ratios of the cavities

The ratio of height and depth of the cavity also affects the air curtain flow. When the H/D ratio varies, the flow nature would be different. As shown in Fig. 6, the thermal insulation is perfectly assured when H/D ratio equals 1.5. When the H/D ratio increases to 2.5, the integrity of the air curtain is destroyed. It may be the reason that, when H/D ratio increases, the stack pressure difference is nearly the same, but the limited inner space of the cavity brings about the entrainment imbalance across the air curtain, and the air flow attaches the inside wall and flow downwards due to the auxiliary transverse pressure difference across the air curtain. When the H/D ratio increases, for the inside limited space the self-generated pressure difference described in eq. (4) has the obvious effect on the flow path of the air curtain. The momentum of the air inside the cavity increases, and the static pressure inside the cavity decreases, therefore the refrigerated air curtain deflects inward. So the Ri number must decrease in order to keep its own flow direction.

Fig. 7 shows the maximum Richardson numbers for combined different H/D and H/b ratios. When the H/D ratio decreases, the maximum Ri number greatly increases, the necessary initial momentum decreases, and the flow stability of the air curtain is then enhanced.

3.3. The effect of discharge angle of the air curtains

As above mentioned, the air curtain flow would deflect inwards due to the pressure difference across the air curtain in

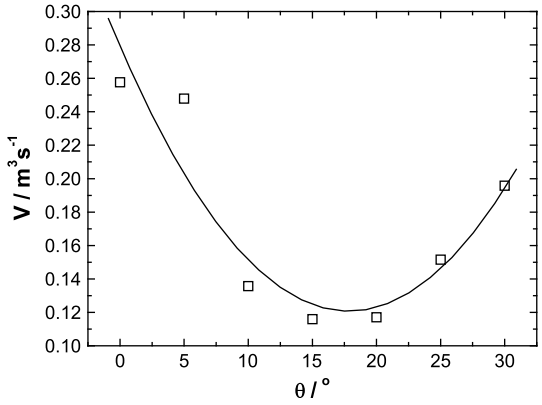

Fig. 9. Volume entrainment rates for different discharge angles (Ri = 0.26, $H/b = 20$).

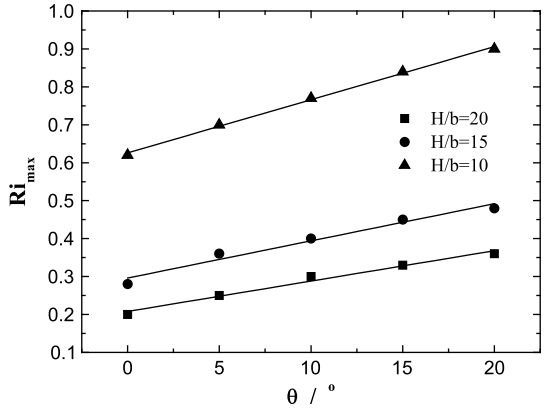

Fig. 10. Maximum Ri numbers for different discharge angles and H/b ratios.

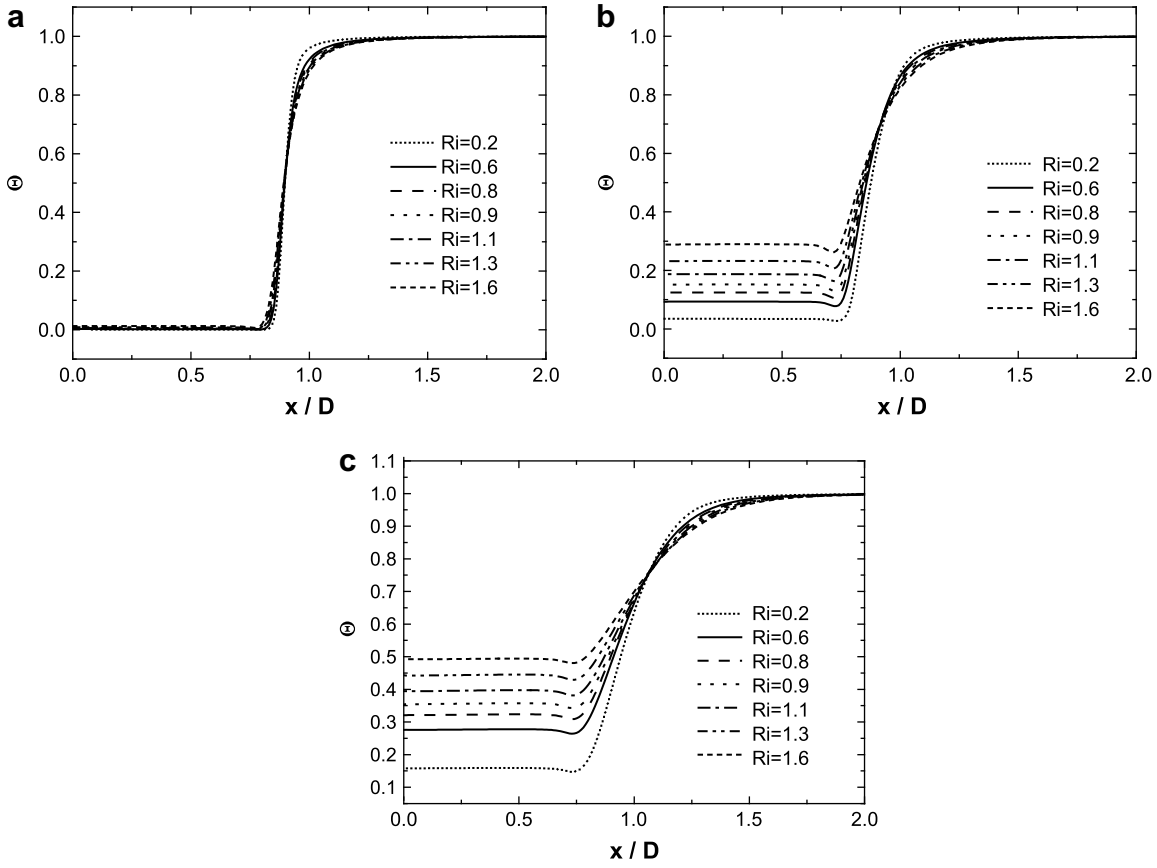

Fig. 11. Temperature distributions at different Ri numbers ($H/b = 20$, $H/D_v = 5$, $D_h/b = 1$): (a) $y/H = 0.9$; (b) $y/H = 0.5$; (c) $y/H = 0.1$.

some cases. Hayes and Stoecker [18] concluded from their research on the non-recirculatory-type air curtain for air doors that the air curtain is less likely to break contact with the floor if the nozzle discharge is directed toward the warm side. So in the same way, it must be useful for flow stability that cold air curtains discharge toward outside to compensate the displacement toward inside the cavity.

When H/b ratio equals 20 and Ri number is 0.26, the vertical air curtain ($\theta = 0^\circ$) cannot work properly as shown in the preceding results. Fig. 8 shows the temperature distributions when the discharge angle changes to 5° and 10° respectively. When the discharge angle increases to 10°, the thermal insulation is assured. So the acceptable range of Richardson numbers widens through varying discharge angles.

But when the discharge angle is too big, the entrainment rate would increase. So definitely there is an optimal discharge angle for each air curtain. Fig. 9 shows volume entrainment rates when Ri is 0.26 and H/b is 20. When θ increases to 10°, the entrainment rate drastically decreases. When the discharge angle increase to 25° and above, the entrainment rate would increase. It is preferred that the discharge angle is 15–20° when other initial parameters are kept unaltered. Fig. 10 shows the maximum Richardson numbers for combined different discharge angles and H/b ratios. The maximum Ri number increases as the discharge angle

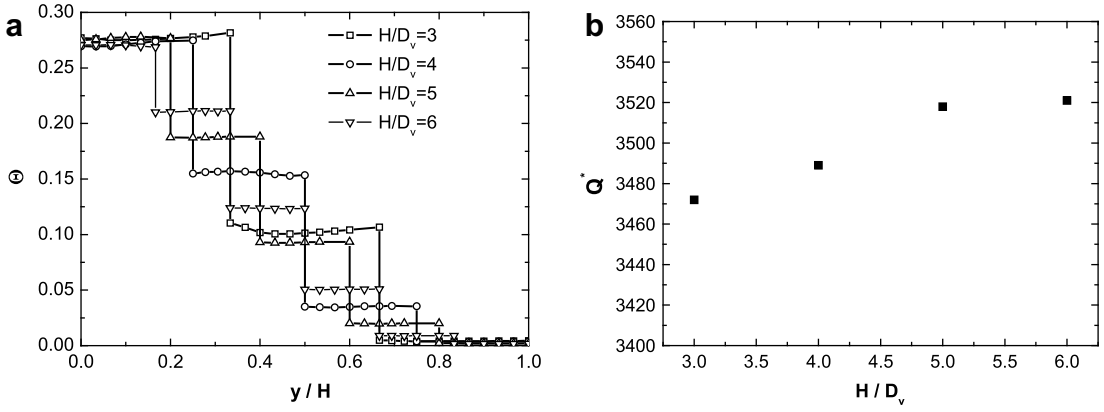

Fig. 12. Temperature distributions (a) and sensible cooling load (b) at different H/D_v ratios (Ri = 0.6, $H/b = 20$, $D_h/b = 1$).

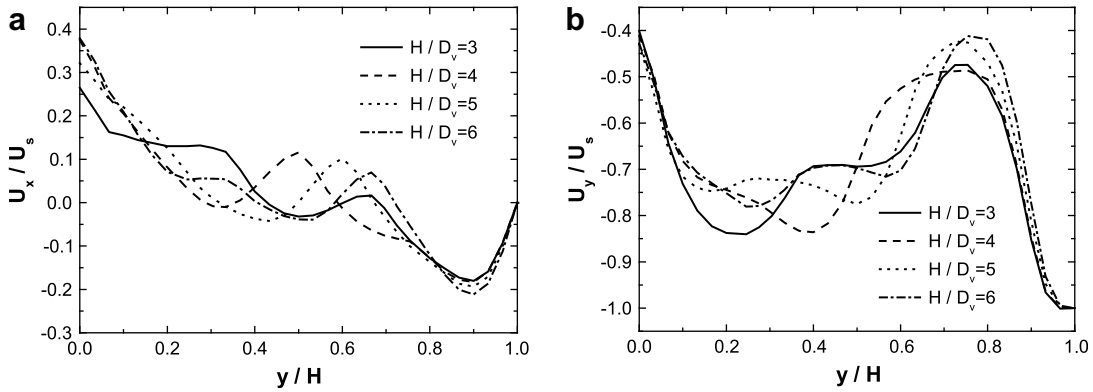

Fig. 13. The transverse velocity (a) and the streamwise velocity distributions (b) along the centerline of the discharge grille at different H/D_v ratios (Ri = 0.6, $H/b = 20$, $D_h/b = 1$).

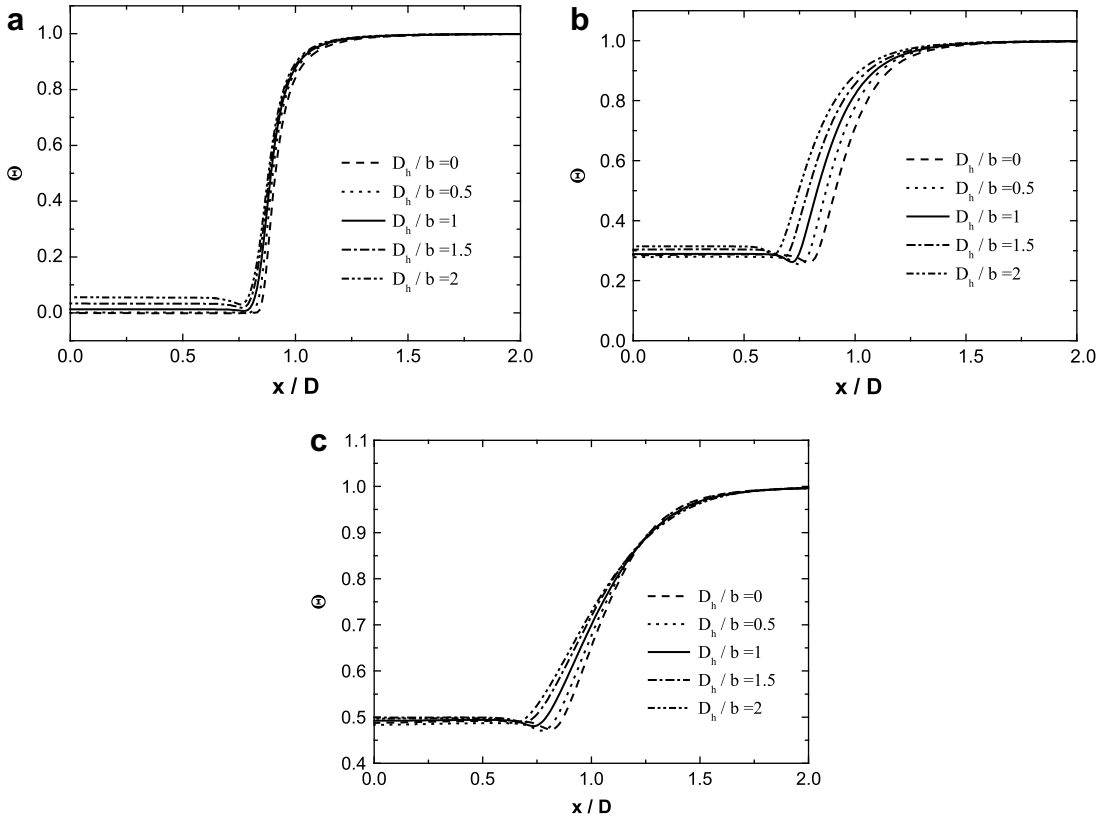

Fig. 14. Temperature distributions at different D_h/b ratios ($H/b = 20$, $H/D_v = 5$, Ri = 0.6) (a) $y/H = 0.9$; (b) $y/H = 0.5$; (c) $y/H = 0.1$.

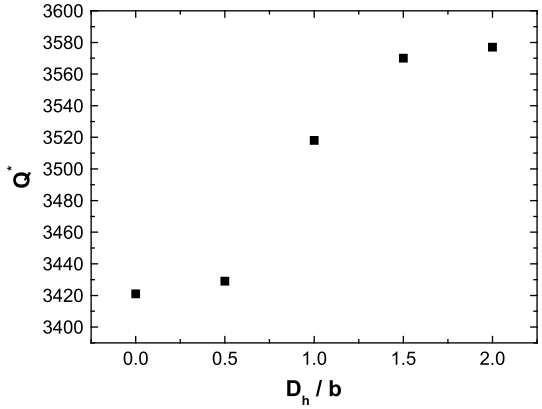

Fig. 15. Sensible cooling load at different D_h/b ratios (Ri = 0.6, $H/b = 20$, $H/D_v = 5$).

increases, and when the H/b ratio decreases, the variation slope slightly increases.

3.4. The effect of the inside shelves

The effect of the shelves is also of great importance for the flow nature and stability of the air curtain. So it is very necessary to study the effect of the shelves. When considering the effect of the shelves, D, b and H are all kept constant, as shown in Fig. 1. Only the D_h or D_v changes respectively. When H/D_v varies, the number of the shelves changes accordingly. When the D_h/b varies, the width of the shelves changes a little.

As shown in Fig. 11, due to the presence of the shelves, the acceptable range of Ri number is relatively large compared with empty cavity, the stability of the air curtain would be enhanced, and the necessarily initial momentum for insulation would remarkably

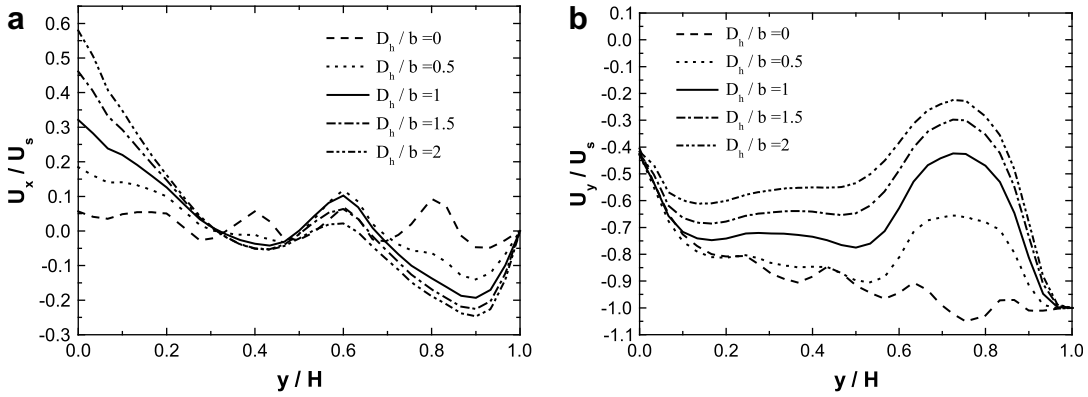

Fig. 16. The transverse velocity (a) and streamwise velocity distributions (b) along the centerline of the discharge grille at different D_h/b ratios (Ri = 0.6, $H/b = 20$, $D_h/b = 1$).

decrease. There are only slight differences in temperature distributions as Ri number changes.

When the H/D_v ratio (i.e. the vertical distances between neighboring shelves) changes, the temperature distributions differs greatly, while the sensible cooling load has only slight differences, as shown in Fig. 12. Fig. 13 shows the transverse and streamwise velocity distributions along the centerline of the discharge grille, which indicates that the variations are very similar for both the transverse and the streamwise velocity. There are only slight differences due to the different positions of the shelves which would cause hindrance or collision with the air curtain flow. The transverse velocity distributions near the return zone are very similar, which indicate D_v has little effect on the entrainment rate of the air curtain, so the sensible cooling load varies a little.

When the D_h/b ratio (i.e. the horizontal distance between discharge grille and shelves) changes, the temperature distribution hardly changes while the sensible cooling load has remarkable differences, as shown in Figs. 14 and 15. When the D_h/b ratio in the range of 0–0.5, the cooling load is smaller. Fig. 16 shows the transverse and streamwise velocity distributions along the centerline of the discharge grille. The transverse velocity distributions near the return zone differ very large, which indicate D_h has great effect on the entrainment rate of the air curtain, so the sensible cooling load varies greatly.

So the vertical distance between the neighboring shelves (D_v) and the horizontal distance between the inner edge of the discharge grille and the front edge of the shelves (D_h) have important effects on the flow and performances of the air curtains. D_v affects the inside temperature distribution and D_h greatly influences the flow direction and cooling load of the air curtains. It is preferable that the ratio of D_h/b is ranging between 0 and 0.5.

4. Conclusions

Thermal insulation performance of recirculated single-band refrigerated air curtains was numerically studied in the present study for design considerations. The results indicate that cold air curtains are negatively buoyant jets, which combine the effects of forced convection and natural convection due to density difference. Cold air curtains flows toward the inside cabinet due to stack pressure, so the initial momentum must be sufficient large to sustain the pressure difference across the air curtain and assure the insulation.

Length–width ratio and discharge angle of air curtains and height/depth ratio of the cabinet would influence the stability of air curtains. Small length/width ratios yield the minimum Reynolds number decreasing (the maximum Richardson number increasing), volumetric entrainment rate reducing and improve temperature distribution and sealing ability. It would be helpful for the sealing stability that air curtains discharge toward outside. The performance of air curtains would be optimal when the discharge angle measured from vertical is in the range of 15–20°.

The effect of shelves inside display cabinets was also studied. The results show that shelves are helpful for flow stability of cold air curtains. The vertical distance between neighboring shelves affects inside temperature distribution and the horizontal distance between the inner edge of the discharge grille and the front edge of the shelves greatly influences the flow direction and the cooling load of air curtains.

The maximum Richardson numbers or the optimum parameter selections in each situation were presented for practical design of single-band air curtains in multi-deck refrigerated display cabinets.

Acknowledgement

This work is supported by the Program for Changjiang Scholars and Innovative Research Team in University (IRT0746).

References

[1] R. Faramarzi, Efficient display case refrigeration, ASHRAE Journal 41 (1999) 46–51.
[2] F.C. Hayes, W.F. Stoecker, Design data for air curtains, ASHRAE Transactions 75 (1969) 168–180.
[3] R.H. Howell, N.Q. Van, C.E. Smith, Heat and moisture transfer through turbulent recirculated plane air curtains, ASHRAE Transactions 82 (1976) 191–205.
[4] R.H. Howell, M. Shibata, Optimum heat transfer through turbulent recirculated plane air curtains, ASHRAE Transactions 86 (1980) 188–200.
[5] D. Stribling, S.A. Tassou, D. Marriott, A two-dimensional computational fluid dynamic model of a refrigerated display case, ASHRAE Transactions 103 (1997) 88–94.
[6] G. Cortella, M. Manzan, G. Comini, CFD simulation of refrigerated display cabinets, International Journal of Refrigeration 24 (2001) 250–260.
[7] P. D'Agaro, G. Cortella, G. Croce, Two- and three-dimensional CFD applied to vertical display cabinets simulation, International Journal of Refrigeration 29 (2006) 178–190.
[8] B.S. Field, E. Loth, Entrainment of refrigerated air curtains down a wall, Experimental Thermal and Fluid Science 30 (2006) 175–184.
[9] R.R. Kalluri, Parametric study of negatively-buoyant wall jets and air curtains, MS Thesis, University of Illinois at Urbana-Champaign, Illinois, 2003.
[10] P. Bhattacharjee, E. Loth, Entrainment by a refrigerated air curtain down a wall, ASME Journal of Fluid Engineering 126 (2004) 871–879.
[11] H.K. Navaz, R. Faramarzi, M. Gharib, D. Dabiri, D. Modarress, The application of advanced methods in analyzing the performance of the air curtain in a refrigerated display case, ASME Journal of Fluid Engineering 124 (2002) 756–764.
[12] H.K. Navaz, B.S. Henderson, R. Faramarzi, A. Pourmovahed, F. Taugwalder, Jet entrainment rate in air curtain of open refrigerated display cases, International Journal of Refrigeration 28 (2005) 267–275.
[13] M. Amin, D. Dabiri, H.K. Navaz, Tracer gas technique, a new approach for steady state infiltration rate measurement of open refrigerated display cases, Journal of Food Engineering (2008). doi:10.1016/j.jfoodeng.2008.10.039.

[14] Y.G. Chen, Research on the flow characteristics and heat transfer of refrigerated air curtains in multi-deck display cabinets, Ph.D. Thesis, Xian Jiaotong University, Xi'an, 2005.
[15] Y.G. Chen, X.L. Yuan, Simulation of a cavity insulated by a vertical single-band cold air curtain, Energy Conversion and Management 46 (2005) 1745–1756.
[16] H.K. Versteeg, W. Malalsekera, An Introduction to Computational Fluid Dynamics – the Finite Volume Method, Longman Scientific & Technical, 1995.
[17] ASHRAE Handbook of Fundamentals: Ventilation and Infiltration, ASHRAE, 2001, (Chapter 26).
[18] F.C. Hayes, W.F. Stoecker, Heat transfer characteristics of the air curtain, ASHRAE Transaction 75 (1969) 153–167.